The Holocene 16,5 (2006) pp. 685–695

Late-Holocene environment and climatic changes in Ameralik Fjord, southwest Greenland: evidence from the sedimentary record

H.S. Møller,[1]* K.G. Jensen,[2] A. Kuijpers,[2] S. Aagaard-Sørensen,[3] M.-S. Seidenkrantz,[3] M. Prins,[4] R. Endler[5] and N. Mikkelsen[2]

([1]Institute of Geography, University of Copenhagen, Øster Voldgade 10, DK-1350 Copenhagen K, Denmark; [2]Geological Survey of Denmark and Greenland, Øster Voldgade 10, DK-1350 Copenhagen K, Denmark; [3]Department of Earth Sciences, University of Aarhus, DK-8000 Århus C, Denmark; [4]Faculty of Earth and Life Sciences, Department of Paleoclimatology & Geomorphology, Vrije Universiteit Amsterdam, De Boelelaan 1085, NL-1081 HV Amsterdam, The Netherlands; [5]Baltic Sea Research Institute, Seestrasse 15, D-18119, Rostock-Warnemünde, Germany)

Received 20 April 2005; revised manuscript accepted 11 January 2006

A HOLOCENE RESEARCH PAPER

Abstract: Sedimentological and geochemical (XRF) data together with information from diatom and benthic foraminiferal records of a 3.5 m long gravity core from Ameralik Fjord, southern West Greenland, is used for reconstructing late-Holocene environmental changes in this area. The changes are linked to large-scale North Atlantic ocean and climate variability. AMS ^{14}C-dating of benthic foraminifera indicates that the sediment core records the last 4400 years and covers the termination of the Holocene Thermal Maximum (HTM). The late HTM (4.4–3.2 ka BP) is characterized by high accumulation rates of fine (silty) sediments related to strong meltwater discharge from the Inland Ice. The HTM benthic foraminiferal fauna demonstrates the presence of well-ventilated, saline bottom water originating from inflow of subsurface West Greenland Current water of Atlantic (Irminger Sea) origin. The hydrographic conditions were further characterized by limited sea ice probably related to a mild and relatively windy winter climate. After 3.2 ka BP lower fine-grained sedimentation rates, but a larger input from sea-ice rafted or aeolian coarse material prevailed. This can be related to colder atmospheric conditions with a decreased meltwater discharge and more widespread sea-ice cover in the fjord.

Key words: Climate change, fjords, sedimentary environment, diatoms, benthic foraminifera, Ameralik Fjord, Greenland, late Holocene.

Introduction

Fjords are the link between the marine and the surrounding terrestrial environment. These inshore waters may provide potentially high-resolution sedimentary records reflecting both terrestrial and marine processes, and thus reveal the history of past climate and environmental change (Syvitski *et al.*, 1987; Gilbert, 2000). Not only local climatic and environmental conditions are reflected in the fjord core records, but these are also influenced by more large-scale changes in the atmospheric and oceanographic regime. It has further been demonstrated that fjord records may provide information on atmospheric and large-scale ocean circulation changes at higher resolution than is generally found in the open ocean (Sejrup *et al.*, 2001; Hald *et al.*, 2003; Lyså *et al.*, 2004). Desloges *et al.* (2002) placed fjords in a climatic continuum using observations of sediment properties and marine/terrestrial controls, with 'most polar' representing the coldest environment. Investigations of

*Author for correspondence (e-mail: hsm@geogr.ku.dk)

10.1191/0959683606hl963rp

the sedimentary fjord environment may thus provide valuable information on palaeoenvironments.

Atmospheric and ocean changes around Greenland affect the dynamics of the Greenland Ice sheet, which controls the drainage and sedimentary input to the fjords. The atmospheric circulation and storm tracks in the West Greenland region are influenced by the position of a tropospheric low-pressure feature, the Baffin Bay trough, which is related to the general circulation system on the Northern Hemisphere (Williams and Bradley, 1985). Oceanographic conditions are controlled by the variability of cold Polar Water advection in the East Greenland Current (EGC) and the warm Atlantic Water from the Irminger Current (IC), which together constitute the West Greenland Current (WGC) (Figure 1). The study area may therefore be well-suited for improving our understanding of the link between changes in atmospheric and oceanographic circulation and smaller-scale, local environmental variability.

The southwest Greenland region where our study area is located (Figure 1) has been demonstrated to be exceptional with regard to Holocene climatic trends observed in most of the Northern Hemisphere. While the Holocene Thermal Maximum (HTM) in most of the northern high latitudes was recorded in the period prior to 7–6 ka BP, terrestrial evidence from southwest Greenland and northeast Canada shows the occurrence of a much later HTM that lasted until 3.5–3.0 ka BP (Kaplan *et al.*, 2002; Kaufman *et al.*, 2004). Moreover, the Godthaabsfjord region around the present study site has been identified as an area where, in the late Holocene, major Neoglacial changes of the inland ice margin occurred (Weidick, 1993).

Investigations of marine sediments and palaeo-environmental records from fjords on Greenland have so far been reported mainly from south and east Greenland fjords (Marienfeld, 1992; Andrews *et al.*, 1994; Jennings and Weiner, 1996; Syvitski *et al.*, 1996; O'Cofaigh *et al.*, 2001; Evans *et al.*, 2002; Jensen *et al.*, 2004; Lassen *et al.*, 2004) while few records exist from west Greenland (Gilbert *et al.*, 1998; Desloges *et al.*, 2002; Lloyd *et al.*, 2005).

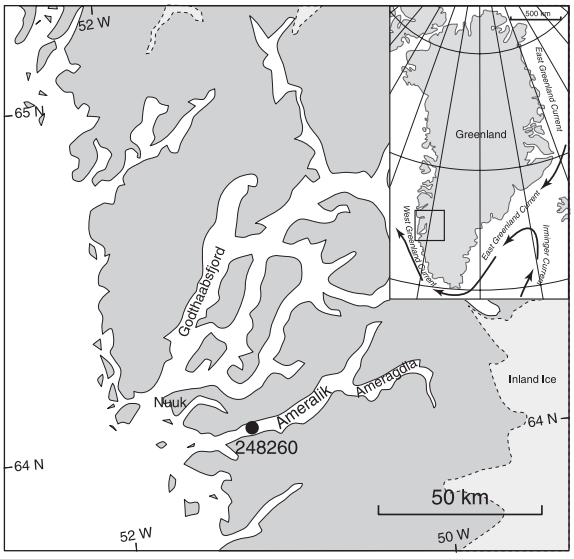

Figure 1 Map of the Godthaabsfjord area with location (solid circle) of the core (no. 248260-2) in the fjord Ameralik. The broken line and the light grey area mark the present position of the inland ice. The inset map shows the regional setting and general ocean circulation around east and south Greenland

This paper presents sedimentological data and micropalaeontological information from Ameralik, one of the fjords in the Godthaabsfjord system near Nuuk, SW Greenland (Figure 1). Based on these data, we discuss environmental changes having occurred in the area during the late Holocene. The objective is to document changes in the marine sedimentary environment, relate these to local climatic changes and improve our understanding of the link between the local hydrographic and climate regime and large-scale North Atlantic ocean and climate variability.

Physiographic setting

The fjord, Ameralik, is a part of the Godthaabsfjord system on the west coast of Greenland (Figure 1). The approximately east–west orientated fjord is 75 km long and 5–7 km wide and is bordered by the 'ice-free' land between the northeastern Labrador Sea and the inland ice margin. The bedrock in this area is part of the Achaean gneiss complex (McGregor, 1993). Mountains ($\sim$1500 m), pronounced cirques and steep valley sides characterize the surrounding landscape. The fjord consists of several deep basins with a maximum water depth of about 700 m, which are separated by shallower sills. At the entrance of the fjord, which is located inshore of the coastal archipelago, a sill is present with a depth of *c.*110 m. Meltwater rivers from outlets of the inland ice drain into the fjord and the rivers of the large delta in front of Ameragdla (Figure 1) contribute 80% of the meltwater to the fjord (Weidick and Olesen, 1980). No calving glaciers are present in the fjord and no icebergs enter the fjord from the open sea. In recent times, sea ice has formed only for brief periods during the coldest winters and with favourable wind (Bennike, 2004).

An estuarine circulation system characterizes the fjord. Cold (1.1°C) and saline (33.3‰) bottom water is found below 200 m depth. The origin of this water mass is the northward-flowing West Greenland Current (WGC), which is a mixture of Polar Water originally derived from the East Greenland Current and Atlantic Water from the Irminger Current (Buch, 2000; Cuny *et al.*, 2002) (Figure 1). Atmospheric heating and meltwater outflow influence the upper water mass, which is less saline (< 31.6‰) and warmer (up to 3.6°C).

Present-day climate (Nuuk, 1961–90) is low arctic with a mean annual temperature of -1.4°C and a mean precipitation of 752 mm (Cappelen *et al.*, 2001). There are marked differences in temperature and precipitation between the coastal area and the interior, with colder and generally drier conditions prevailing in the interior (Taurisano *et al.*, 2004). Major cyclone systems normally approach the area from the southwest. Strong winds may occur in the fjord, especially during fair weather in winter when katabatic winds blow from the inland ice towards the open sea.

Quaternary terrestrial deposits in the valley system are limited to glaciofluvial deposits at the head of Ameragdla (Figure 1), whereas moraines and raised marine deposits can be observed in minor valleys along the fjord side (Weidick, 1978). In postglacial times the inland ice margin retreated gradually from the outer coast (*c.* 10 ka BP) to a position *c.* 10 km inland of the present ice margin around 4 ka BP (Weidick, 1993). The subsequent Neoglacial re-advance culminated with the 'Little Ice Age' limit near the present ice margin (Funder, 1989). Emergence curves for the Godthaabsfjord area suggest that present sea level was reached 3–4 ka BP, followed by a submergence (Weidick, 1993). Archaeological investigations support the geological evidence of submergence during the last

millennium as some of the Norse (*c.* AD 1000–1360) ruins in the Ameralik Fjord are found below sea level (Roussell, 1936). Further to the north in the Disko Bugt area (69°N) a corresponding history of sea-level changes has been recorded with up to 3 m relative sea-level rise during the last two millennia (Rasch, 2000; Long *et al.*, 2003).

Methods

The 348 cm long gravity core (248260-2) was collected in 2002 during a cruise with R/V *Alexander von Humboldt*. The coring site (64°5.433′N; 51°15.530′W) is located in 674 m water depth landward of the outer main sill in the fjord (Figure 1). Wet bulk density (g/m^3) on the whole core and magnetic susceptibility (SI-units) on the spilt core were determined in 0.5-cm steps using a multisensor core logging system (Weber *et al.*, 1997). The split cores were visually logged and scanned using a RGB colour scanner, X-rayed and subsampled. The bulk geochemical composition was determined using an X-ray fluorescence (XRF) core scanner in 1-cm steps by measuring in 30 s at 10 kV (Jansen *et al.*, 1998). XRF logging data are semi-quantitative but produce reliable down-core estimates of the elemental composition (Jansen *et al.*, 1998). The intensity of the elements Fe and Ca are included in this study and reported as counts per second. The total carbon content (%) was analysed on freeze-dried samples using an ELTRA CS-500 Analyser. The grain size (< 2 mm) was determined on non pre-treated, dispersed and sieved samples using a laser particle analyser (Malvern Mastersizer). The identification of particles larger than 2 mm and interpretation of sedimentary structures were based on X-radiographs. End-member modelling algorithms are applied on the grain size data to obtain independent grain size distributions of the different types of sediment (Weltje, 1997). The end-member method facilitates the distinction and quantification of subpopulations within grain-size distribution data (Weltje and Prins, 2003).

Detailed information on laboratory processing and interpretation of the benthic foraminiferal and diatom data is presented in (M.-S. Seidenkrantz, S. Aagaard-Sørensen, H.S. Møller, A. Kuijpers, K.G. Jensen and H. Kunzendorf, unpublished data 2006). Samples for analyses of the benthic foraminiferal fauna were collected as 1-cm core slices at 2 cm or 3 cm intervals in the upper 112 cm (3.2 ka BP) and at 10 cm intervals below. The sampling intervals for diatom analyses were 4 cm in the upper 1 m (*c.* 3 ka BP) of the core and 8 cm interval in the remaining lower part.

Age model

The age control of gravity core 248260-2 is based on Atomic Mass Spectrometry (AMS) ^{14}C measurements, carried out on material from gravity core 248260-2 at the AMS ^{14}C Laboratory, University of Aarhus, Denmark. Five samples were measured for their ^{14}C content. Benthic foraminifera were used for dating on four of these samples. Dating of one of these samples (AAR-9054) was based on measurements of monospecific *Elphidium excavatum* f. *clavata*; the other three samples were composed of a mixed assemblage (Table 1). When picking the specimens for dating, care was taken to choose only well-preserved specimens, thus diminishing the risk of contamination. In addition to the four samples consisting of benthic foraminifera, one mollusc fragment, presumably belonging to the species *Yoldia hyperborea*, was dated (AAR-9221). However, the mollusc fragment showed signs of post-depositional transportation (S. Funder, personal communication 2004) and, as it yielded an older age than the foraminiferal fauna just below (Table 1), the age of the mollusc fragment was disregarded in the age model.

The bottom water of the Ameralik fjord is today washed by Atlantic-source, subsurface waters from the West Greenland Current, therefore we applied a standard reservoir correction of 400 years to all results ($\Delta R = 0$) (Table 1). The ^{14}C ages were calibrated using the OxCal v. 3.9 program (Bronk Ramsey, 2001) and the marine calibration dataset MARINE98 (Stuiver *et al.*, 1998), and the age model is based on the median values of the calibrated dates and linear interpolation (Telford *et al.*, 2004) (Table 1). A linear sedimentation rate was assumed between the dated levels (Figure 2). Based on the datings there is a significant change in sediment accumulation rate around 1 m core depth. A significant change in sediment composition (see Figures 2 and 4) and foraminiferal assemblages (see Figure 5) at 107 cm core depth, where no dating is available, marks a significant change in sedimentary regime, and presumably also in sedimentation rates (Figure 2). With a dating available at 97.5 cm depth, the sedimentation rate for the 107 to 97.5 cm interval is inferred to be similar to the rate from the dated layer above (97.5–60 cm). A turbidite-like interval (93–95 cm, see below) is excluded from these calculations. We thus place the change in sedimentation rate at 107 cm depth, which provides an age of *c.* 3.2 ka BP for the major change in sedimentary environment. Using this age model each 1 cm of sediment represents between 5 and 42 calender years.

Table 1 Radiocarbon dates from core 248260-2, Ameralik, Greenland

Depth (cm)	Lab. no	Sample type	^{14}C age (BP)	Res. corrected ^{14}C age (BP)	Calibrated age BP (1 &2 σ ranges)	Median calibrated age (BP)
20	AAR-9221	Mollusc fragment[a]	1039 ± 39	639 ± 39	640–565 670–540	605
21–24	AAR-9265	Benthic forams	984 ± 40	584 ± 40	610–535 640–510	575
58.5–62	AAR-9266	Benthic forams	1865 ± 49	1465 ± 49	1470–1340 1520–1300	1400
95–100	AAR-9054	*Elphidium excavatum* f. *clavata*	3013 ± 49	2613 ± 49	2835–2740 2890–2710	2780
330–345	AAR-9055	Benthic forams	4260 ± 55	3860 ± 55	4430–4280 4510–4190	4360

All ^{14}C-ages are calibrated to calendar years (cal. yr BP) using OxCal v.3.9 calibration program (Bronk Ramsey, 2001) and the marine model calibration curve (MARINE98, Stuiver *et al.*, 1998) with a standard marine reservoir correction of 400 years. Median calibrated ages are used in the age model assuming linear sedimentation rates between intervals.

[a]Redistributed shell fragment presumably *Yoldia Hyperborea*, not used for the age model.

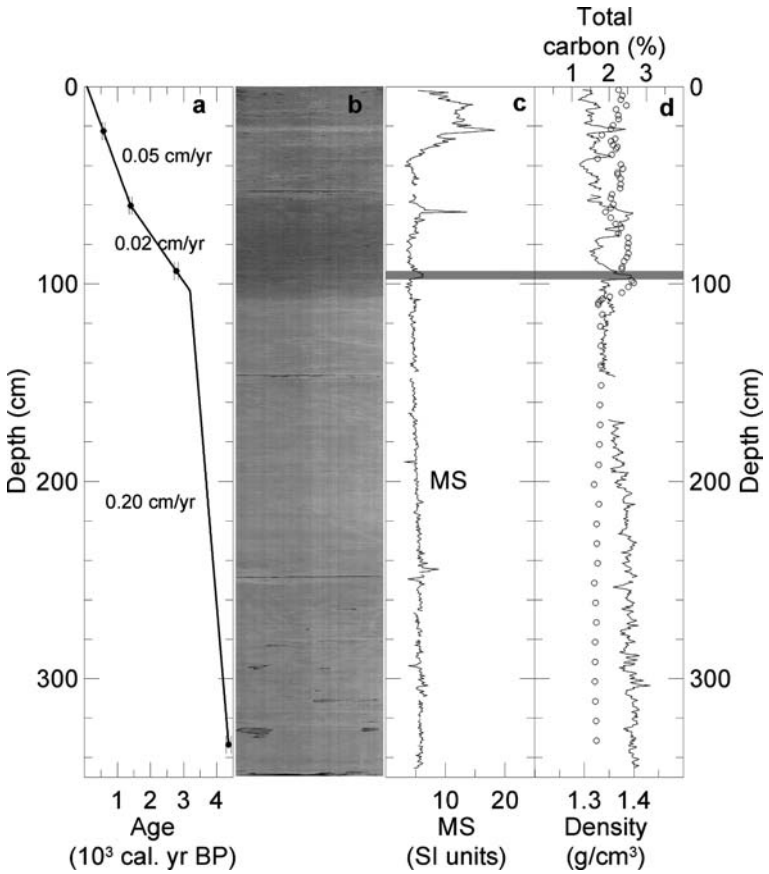

Figure 2 Core 248260-2 showing (a) the age model and sedimentation rate based on radiocarbon dates, (b) black and white image of colour scanning of split core surface, (c) magnetic susceptibility and (d) wet bulk density from MSCL-scan (line) and total carbon content (open circles). The shaded interval indicates the turbidite disregarded in the age model

Results

Core lithology and magnetic susceptibility

The core contains fine-grained, homogenous (silty) sediments with indications of bioturbation mainly in the lower part. The only exception is the 95–93 cm interval, which displays evidence of a turbiditic, fast sedimentation episode as revealed on X-radiographs. A discrete peak in the magnetic susceptibility and wet bulk density may support this interpretation (Figure 2). The sediment colour is olive grey to light olive grey with scattered small black spots; in the upper 1 m the sediment is darker (olive grey) than the rest of the core (light olive grey). Magnetic susceptibility values are consistently low from the bottom of the core to 40 cm depth (Figure 2c). An increase is observed upward from a depth of *c*. 40 cm, reaching maximum values at 22 cm, which is again followed by a gradual decrease toward the core top. Wet bulk densities range from 1.29 to 1.43 g/cm^3, with the largest variations in the upper 1 m of the core (Figure 2d). Stable values and a slight down-core increase in density characterizes the lower part of the core. Total carbon content in the core ranges between 1.6 and 2.7% (Figure 2d). The total carbon content is relatively low and stable below 107 cm (mean, $\chi = 1.7\%$, standard deviation, $\sigma = 0.07\%$); above this level it is higher and more variable ($\chi = 2.2\%$, $\sigma = 0.21\%$). Analyses of selected samples show that around 65% of the total carbon is organic carbon and that C/N-ratios are around 5–7, the latter documenting a marine origin of the organic matter.

Accumulation rates, grain-size and geochemical properties

Average sediment accumulation rates range from 24 to 197 cm/ka, which implies a chronological resolution of 5–42 y/cm of sediment (Figure 2a). There are no indications of disturbance of the core top of the gravity core and ^{210}Pb dating of a supplementary box core supports the estimated average sediment accumulation rates of 0.05 cm/yr in the upper layers (M.-S. Seidenkrantz, S. Aagaard-Sørensen, H.S. Møller, A. Kuijpers, K.G. Jensen and H. Kunzendorf, unpublished data 2006).

The samples are fine grained with mean grain sizes between 5 and 16 μm (Figure 3a). The grain-size distribution of the dispersed samples is often bi-modal and very poorly sorted (Figure 3). The grain-size spectrum is dominated by up to 60–70 vol.% silt (2–63 μm). The upper 1 m (3–0 ka BP) of the core has a greater content of sand (up to medium to coarse sand) and includes intervals with particles larger than 2 mm (Figure 4b). The mean grain size is positively correlated with sorting; samples with coarser mean grain size are more poorly sorted (Figure 3a). The end-member modelling algorithm was applied to the data set of grain size distributions ($n = 44$) (Weltje, 1997). The modelling results indicate that the sediments can be described as a mixture of three end-members (Figure 3c). The three-end-member model explains 77% of the variance ($r^2 = 0.77$). Two of the end-members (EM1 and EM2) have marked sand-sized modes while the third end-member (EM1) is characterized by clay and silts (Figure 3c). Between the base of the record (4.4 ka BP) and 3.2 ka BP the fine-grained end-member (EM1) dominates (Figure 4a). During the remaining period the influence from the two sandy end-members (EM1 and EM2) in the sediment is generally higher and with larger variation (Figure 4a).

Geochemical properties are presented in Figure 4. The intensity of calcium (Ca) ranges between 210 and 400 counts per second (cps) and are highest in the lower part and in the very upper part. Major variations in the calcium intensity occur at about 3.2, 2.7 and 0.8 ka BP (107, 93 and 32 cm,

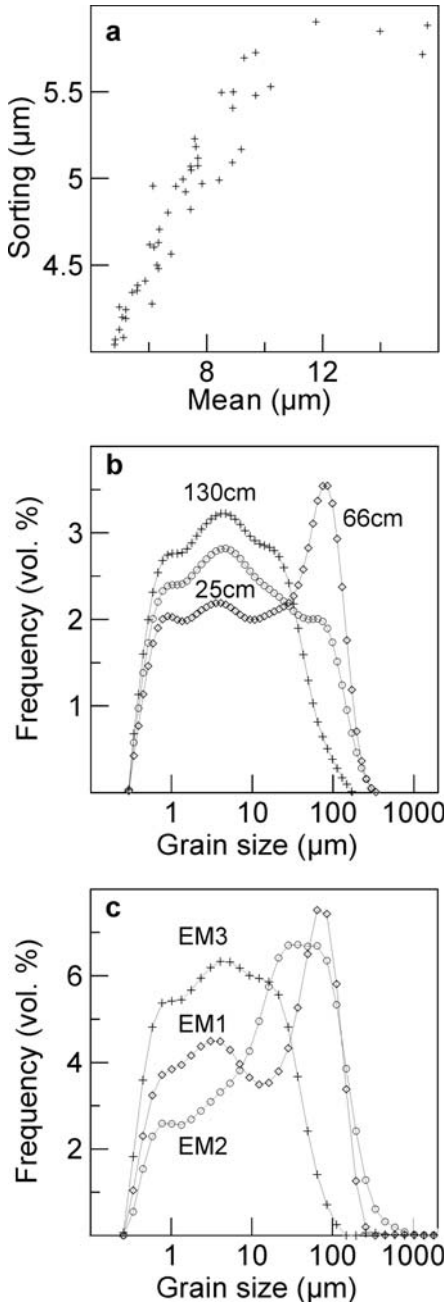

Figure 3 Grain size characteristics: (a) mean grain size versus sorting, (b) three examples of characteristic grain size distributions from 25 cm, 66 cm and 130 cm depth, and (c) the end-member modelling results according to the three-end-member model

respectively). The intensity of iron (Fe) is between 650 and 860 cps and the variations correspond to some extent to the Ca variations (Figure 4c). A larger interval of higher Fe counts characterizes the lower part of the core (> 3.2 ka BP), while minimum values occur near the core top (< 0.5 ka BP).

Benthic foraminifera and diatoms

The benthic foraminiferal fauna is generally characterized by shifts between intervals with dominantly calcareous taxa such as *Elphidium excavatum* forma *clavata* Cushman, *Cassidulina reniforme* Nørvang, *Astrononion gallowayi* Loeblich and Tappan, *Cibicides lobatulus* (Walker and Jacob) and *Islandiella helenae* Feyling-Hansen and Buzas, and intervals where the fauna almost exclusively consists of agglutinated species (eg, *Deuterammina ochracea* (Williamson) and *Verneuilina arctica* Höglund) (Figure 5). These calcareous taxa are commonly found in modern arctic shelf seas and outer fjords at salinities > 33‰ (Steinsund, 1994; Jennings and Helgadottir, 1994; Hald and Korsun, 1997; Polyak *et al.*, 2002) and the faunas resemble those found in other fjord cores from south and west Greenland (Øhlenschlæger, 2000; Lassen *et al.*, 2004).

Between 4.4 and 3.2 ka BP the concentration of foraminifera (number per gram) is low and the fauna is dominated by a calcareous species (Figure 5). A change to an agglutinated fauna just after 2.7 ka BP is preceded by a marked increase in the concentration of the calcareous foraminifera *Elphidium excavatum* forma *clavata* (3.2–2.7 ka BP). Generally the agglutinated foraminifera dominate between 2.7 and 0.8 ka BP, with a clear minimum around 1.4 ka BP. This is followed by a period from 0.8 ka BP to present with relatively high numbers of primarily calcareous foraminifera.

The diatom flora is dominated by taxa characteristic of arctic waters and sea-ice habitats, with minor influences from Atlantic/non-arctic species. The dominant species are *Thalassiosira nordenskioeldii* Cleve, *Fragilariopsis oceanica* (Cleve) Hasle, *Fragilariopsis cylindrus* (Grunow) Krieger, and *Chaetoceros furcellatus* Bailey resting spores. Unidentified *Chaetoceros* resting spores which dominate the planktic diatom flora throughout the core with abundances of 200–600% of the remaining diatom flora (not shown), are not included in the percentage calculations. The benthic flora contributes a significant number of valves between 5 and 25% (Figure 5). The relative abundance of the species *Thalassiosira nordenskioeldii* increases at 3.1 ka BP (106 cm) and decreases again at 1.1 ka BP (48 cm) while the relative abundance of sea-ice associated species is relative constant throughout the record with an increase at 0.8 ka BP (30 cm) (Figure 5).

Discussion

Sediment supply and dispersal within the fjord basin are affected by glacial processes, fluvial conditions, topography, bathymetry, sea level, hydrography of coastal waters, and climate (Syvitski *et al.*, 1987; Forbes and Syvitski, 1994). The major processes that govern sediment supply to an arctic fjord are: settling of suspended plume sediments from meltwater; turbidity currents and debris flow; rafting from icebergs and sea ice; aeolian transport; and reworking of deltas and outwash terrains resulting from glacial isostatic recovery (Gilbert, 1983; Andrews and Syvitski, 1994). The influence from settling of suspended sediment from fluvial plumes is generally considered an order of magnitude more important than the other processes (Andrews and Syvitski, 1994). Though the various factors and processes may interact and dominate at different times and on different timescales, the major factor controlling these processes is climate (Syvitski *et al.*, 1987; Andrews and Syvitski, 1994; Ballantyne, 2002). Numerical models of the sedimentary processes show that slowly changing climate may lead to abrupt changes in the sedimentary environment (Morehead *et al.*, 2001). Analyses of sedimentary properties and structures in fjord sediments aid identification of the different sedimentary processes and modes of deposition (Stravers *et al.*, 1991; O'Cofaigh and Dowdeswell, 2001).

The studied core represents the last 4.4 ka and reveals a number of changes in the sedimentary fjord environment that indicate significant hydrographical and climatic changes. The grain-size data and supplementary clay mineral analysis from the core identify the sediment as locally derived glacial flour (H. Lindgreen, personal communication, 2004). This is confirmed by analysis of the isotopic composition of sediment

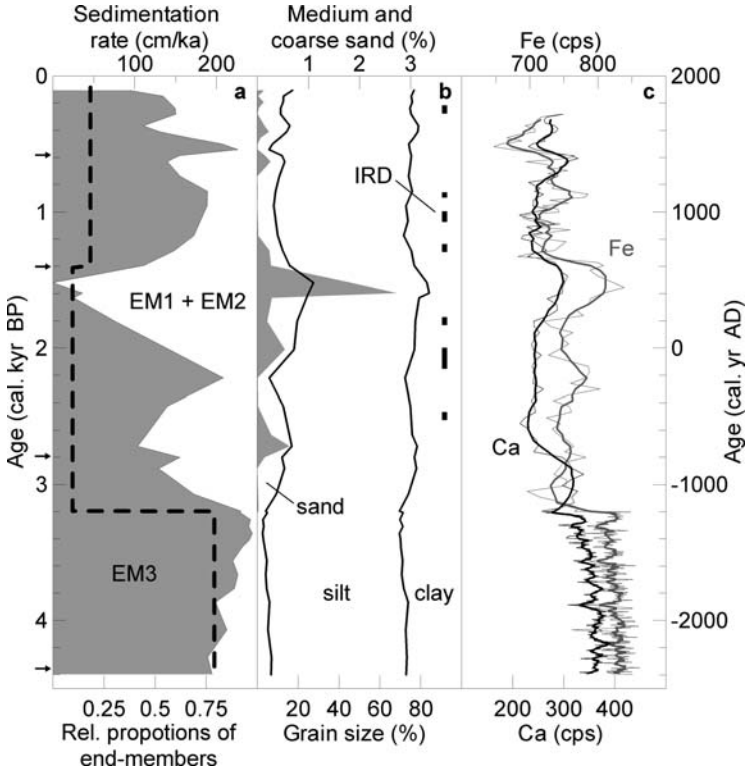

Figure 4 Logs of sedimentary parameters versus age, (a) sedimentation rate and the relative proportion of coarse end-members (EM1 + EM2) and the fine-grained end-member (EM3), (b) content of sand, silt and clay (solid lines), content of medium and coarse sand (filled area on exaggerated upper scale) and the occurrence of material >2 mm (vertical black bars), and (c) XRF intensity of iron (Fe) and Calcium (Ca) in 0.5-cm steps and 5-cm running average. Arrows at the left of (a) indicate position of radiocarbon dates

from the fjord, which also identifies a local provenance for the material (van de Flierdt *et al.*, 2005). Magnetic susceptibility (MS) and variations in MS are a function of changes in provenance, in the inputs of detrital carbonates and organic carbon, and grain size of the constituent magnetic minerals (Andrews and Stravers, 1993; Stoner and Andrews, 1999). Uniform low MS values through the core support the interpretation of a consistent regional geological provenance of the sediment. Minor variation in the upper 1 m in MS may be attributed to changes in grain size or organic carbon content (Figures 2 and 4).

Fe, Ti, K and Si are common elements in the surrounding bedrock (Steenfelt, 1990) and constitute 70–80% of the elements in the XRF-analyses. The intensity of iron (Fe) from the XRF-scanning is used as an indicator of the influence from terrestrial material. No widespread calcium-bearing rocks occur in the area (McGregor, 1993), thus the variation in the Ca-intensity from the XRF-scanning must indicate variation in

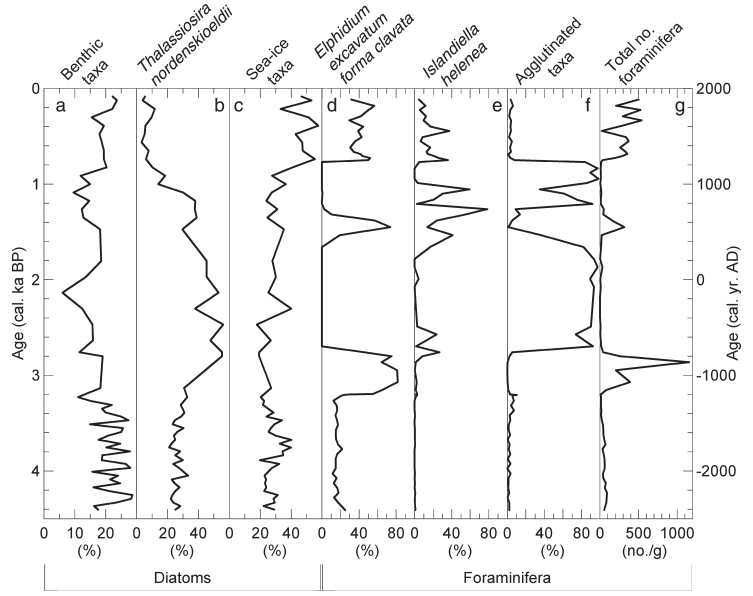

Figure 5 The relative abundance of (a) benthic diatom species (%), (b) the neritic-boreal diatom *Thalassiosira nordenskioeldii* (%), (c) sea-ice associated diatom assemblage (%), (d) the opportunistic foraminifera *Elphidium excavatum* forma *clavata* (%), (e) the foraminifera *Islandiella helenae* (%), (f) agglutinated foraminifera (%), and (g) the total number of benthic foraminifera per gram sediment. Note different scale on curves

the marine production and biogenic calcium input relative to the input of terrestrial material. Ca-intensity has previously been calibrated to measured calcium carbonate content in marine environments (Jansen *et al.*, 1998; Prins *et al.*, 2001). The period from 4.4 to 3.2 ka BP and three shorter periods in the last 3.2 ka BP (3.2–2.7 ka BP; 1.6–1.2 ka BP; 0.8–0.3 ka BP) have increased intensity of Ca superimposed on a background Ca signal (250 cps). The latter three intervals correspond with intervals of high numbers (number/gram) of calcareous benthic foraminifera (Figure 4c and 5g) while the amount of foraminifera (number/gram) during the 4.4–3.2 ka BP interval is concluded to be diluted by the high input of terrestrial material. This supports the interpretation of Ca as an indicator of variation in the marine production of biogenic calcium.

The large proportion of fine-grained glacial flour (Figure 4) is typical for fjord environments and the clay and silts may be ascribed to settling of suspended plume sediments from meltwater (Syvitski *et al.*, 1987). Direct meltwater input is recognized as one of the primary pathways of sediment delivery to fjords on west Greenland (Gilbert *et al.*, 1998). Suspension transport of coarser material in meltwater plumes such as sand over long distances is impossible; the presence of sand may thus be ascribed to alternative sedimentation processes such as rafting from sea ice/icebergs, aeolian processes or turbidites and debris flow. Except for one minor interval (95–93 cm) there are no indications of turbidites and debris flow deposits in the sediment core. Since no marine-ending glaciers have terminated in the fjord during the documented period (4.4 ka) (Weidick, 1993) and no icebergs enter the fjord from the sea, rafting from icebergs can also be disregarded as a major process of sedimentation in Ameralik. Rafting from sea ice and aeolian processes are thus the most likely processes responsible for deposition of sand. In recent times, sea ice has occured briefly in the fjord during the coldest winters and favourable wind conditions (Bennike, 2004). Aeolian processes may be a significant primary source of sandy sediment in arctic fjord environments (Neuman, 1993). Furthermore, sandy aeolian sediment may also act as source material to the sea ice, together with littoral, colluvial and fluvial sources (Gilbert, 1990).

The results from the end-member modelling support the identification of independent sediment transport mechanisms. The fine-grained end-member (EM3) may resemble the fine-grained result of suspension settling of sediment from a turbid surface meltwater plume. The two end-members with marked coarse grained modes (EM1 and EM2) may be attributed to sea-ice rafted or aeolian material. The relative contribution of the fine-grained end-member (EM3) is an indication of the importance of suspension settling as a sedimentation process and the coarse-grained end-members (EM1+EM2) may thus be a proxy for sea-ice rafting or aeolian processes.

Interval 4.4–3.2 ka BP

The lower part of the core covering the period from 4.4 ka BP to 3.2 ka BP displays little variation in sedimentological properties with relatively small variations in the magnetic susceptibility, density and total carbon content (Figure 2). This suggests a period with a stable sedimentary and hydrographic regime. The period is characterized by high sediment accumulation rate, high Ca and Fe intensities, high proportions of the fine-grained end-member (EM3), no particles larger than 2 mm and only minor sand content (Figure 4).

The large quantity of fine-grained sediment is interpreted as originating from melting of land-based outlets of the inland ice in the drainage area. The sediment is transported down-fjord in the turbid surface plume. Analogous sediment transport scenarios with significant sedimentation from turbid surface plumes have been observed under present-day conditions, for example in fjords on Disko and Baffin islands (Winters and Syvitski, 1992; Gilbert 1998, 2002) and are evident on satellite images of the west coast of Greenland. Studies from fjords on east Greenland show that meltwater transport, deposition and flux of fine-grained sediments is significant even in high arctic glacimarine environments (O'Cofaigh *et al.*, 2001). The sand-sized materials indicate aeolian activity or the presence of sea ice in the fjord.

The benthic foraminiferal assemblage in this period is a diverse, calcareous (agglutinates $< 10\%$) fauna dominated by *Cassidulina reniforme*, *Astrononion gallowayi*, *Cibicides lobatulus* and *Elphidium excavatum*, forma *clavata* (Figure 5 and M.-S. Seidenkrantz, S. Aagaard-Sørensen, H.S. Møller, A. Kuijpers, K.G. Jensen H. Kunzendorf, unpublished data 2006) The diatom assemblage is dominated by the planktonic taxa *Thalassiosira nordenskioeldii*, *Fragiolariolopsis cylindricus* and a high influx of benthic taxa. The microfossil data indicate an arctic high-energy environment with cold, stable bottom-water, salinities of $> 33‰$ (Steinsund, 1994; Polyak *et al.*, 2002), which can be linked to an influx of WGC water of Atlantic (Irminger) origin to the fjord bottom. The data further suggest the presence of some winter sea ice in the region at least during the severe winters (M.-S. Seidenkrantz, S. Aagaard-Sørensen, H.S. Møller, A. Kuijpers, K.G. Jensen H. Kunzendorf, unpublished data 2006). The strong surface meltwater outflow may also have been responsible for an enhanced inflow of saline waters to the bottom of the fjord as a part of the estuarine circulation process. The content of total carbon is very constant during the period and, despite dilution by the influx of terrestrial inorganic material, the record shows relatively high values when compared with other arctic fjord environments (Syvitski *et al.*, 1990). This supports the interpretation of high marine biological activity as inferred from the Ca-intensity and the microfossil assemblages.

The high sediment accumulation rate of fine-grained sediments, which is related to strong meltwater discharge from the inland ice, and the limited sea-ice cover indicate a relatively warm, and possibly windy atmospheric climate.

The described period of relatively warm atmospheric conditions at Ameralik (4.4–3.2 ka BP) coincides with the late phases of the period between 6.3 and 3.5 ka BP, which is identified as the warmest and driest period of the Holocene in the Godthåbsfjord interior (Fredskild, 1983). The period is furthermore described as the late stage of the Holocene Thermal Maximum (HTM) in the Labrador region (Kaufman *et al.*, 2004). The characteristics of the HTM across Greenland demonstrate that warming was generally more pronounced in southwest Greenland and at lower elevations, particularly near the coast (Kaufman *et al.*, 2004). Sea-surface temperatures up to 2–3°C warmer than present were reconstructed for the East Greenland Current for the 6.5–3.0 ka BP interval (Andersen *et al.*, 2004) suggesting favourable conditions for a warmer mid-Holocene WGC as well. Records of Holocene aeolian activity in west Greenland demonstrate that the period prior to c. 3.5 ka BP was characterized by increased aeolian activity (Willemse *et al.*, 2003). This may support the recognition of sand as an indicator of aeolian activity and implies unfavourable conditions for the formation of an extensive sea-ice cover. The core record thus shows the termination of the HTM at 3.2 ka BP at the same time as indicated by recent ice core temperature reconstruction (Vinther *et al.*, 2005), but the

beginning of the HTM can not be documented by our study because of shortness (4.4 ka BP) of the present record.

Interval 3.2 ka BP – present

When compared with the preceding period, several changes in lithological parameters and microfossil content indicate more unstable environmental and hydrographic conditions during the past 3.2 ka. The sediment accumulation rate is significantly lower and the amount of coarse-grained material (> 63 μm) increases from around 3.2 ka BP (Figure 4). Material larger than 2 mm is also observed in this interval and the proportion of the coarse-grained end-members (EM1 + EM2) are higher.

This indicates a decreased deposition of terrestrial, fine-grained sediment from meltwater outflow. The input of coarse material (> 2 mm) show the presence of sea-ice. A general atmospheric cooling of the area, resulting in a decreased ablation of the inland glaciers and more frequent sea-ice formation may be responsible for this. Sediment discharge in arctic rivers is sensitive to air temperatures in the drainage basin, with decreasing sediment load at lower temperature (Syvitski, 2002). A similar, climate-controlled response in fjord sedimentation has been recognized in the marine environment along the western Antarctic Peninsula (Domack *et al*., 2003) and in numerical models of sediment discharge and accumulation to a fjord during the Holocene (Morehead *et al.*, 2001).

The lower sedimentation rates and lower iron intensity (Figure 4) provide evidence of decreased meltwater production. The percentage of total carbon increased during this period (Figure 2), which can be ascribed to reduced dilution by inorganic terrestrial material rather than increased marine biogenic productivity. This interpretation is supported by generally lower Ca-intensity in the period, which suggests limited marine productivity. A marked decrease in Ca-intensity at 3.2 ka is followed by a renewed increase towards 2.7 ka BP, coinciding with a larger concentration of calcareous foraminifera (Figure 4c and 5g). An initial change towards colder climatic conditions and associated meltwater reduction can be assumed to have not only affected local hydrographic conditions in the fjord, but presumably also led to large-scale changes in (west) Greenland coastal waters and regional ocean circulation patterns, simultaneously affecting marine (micro-) flora and fauna.

The opportunistic *Elphidium excavatum* forma *clavata* initially replaces the diverse, calcareous fauna found prior to 3.2 ka BP. Just after 2.7 ka BP the calcareous, benthic foraminiferal fauna disappears altogether, leaving only an assemblage of agglutinated species (Figure 5f). This indicates the development of unfavourable bottom-water conditions, hostile to calcareous taxa (M.-S. Seidenkrantz, S. Aagaard-Sørensen, H.S. Møller, A. Kuijpers, K.G. Jensen H. Kunzendorf, unpublished data 2006). The dominance of the agglutinated foraminiferal assemblages coincides with the occurrence of coarse sea-ice-rafted material (Figure 4b and 5f). Apart from short intervals with blooms of *Elphidium excavatum* forma *clavata* and *Islandiella helenae*, the agglutinated fauna dominates the foraminiferal assemblages between *c*. 2.7 and 0.8 ka BP (*c*. 700 BC–AD 1200). During this time period, denser (saline) WGC water had only little influence on the bottom water masses of the fjord. An increase in frequency of the diatom species *Thalassiosira nordenskioeldii* during 3.2–1.1 ka BP (Figure 5b) may, however, indicate continued inflow of (low-salinity) WGC surface water into Ameralik Fjord. The occurrence of sea-ice-associated diatom species and *Islandiella helenae* show the presence of at least seasonal sea-ice cover during this period (Figure 5c and e) (M.-S. Seidenkrantz, S. Aagaard-Sørensen, H.S. Møller, A. Kuijpers, K.G. Jensen H. Kunzendorf, unpublished data 2006).

The low sediment accumulation rate of fine-grained sediments and the occurrence of ice-rafted material indicate a relatively cold atmospheric climate and possibly also decreased wind activity favouring the presence of more widespread sea ice.

The timing of the cooling at 3.2 ka BP corresponds to the initiation of the Neoglacial glacier advances around 3.5–3 ka BP in the area (Kelly, 1980) and a widespread pronounced cooling around the Labrador Sea (Kaufman *et al.*, 2004). Pollen curves from a lake within the Godthåbsfjord drainage system indicate a gradual decrease in temperature from 3 ka BP (Fredskild, 1983). Marked cooling from 3 ka BP, followed by unstable conditions during the rest of the Holocene, is recorded in several lake records south of the present study site (Funder and Fredskild, 1989; Kaplan *et al*., 2002; Kerwin *et al*., 2004). In a sediment core from Disko Fjord, west Greenland (69°N), the foraminiferal assemblages change from a calcareous to a dominantly agglutinated fauna at *c*. 2.9 ka BP, thus also indicating a change to colder conditions (Øhlenschlæger, 2000). No records of sea-surface temperatures exist from offshore west Greenland for this period. However, the observed cooling coincided with a temperature lowering in the East Greenland Current observed during the last 3 ka BP (Figure 6c) (Jennings *et al*., 2002; Andersen *et al*., 2004). Furthermore ice-core data identify the time of 3.2 ka BP as the beginning of a late-Holocene cooling trend (Vinther *et al*., 2005), this is documented by other studies that also report increasing snow accumulation (Cuffey and Clow, 1997; Dahl-Jensen *et al.*, 1998).

Renewed appearance of the calcareous foraminifera and an increase in the relative abundance of sea-ice associated diatoms are observed at about 0.8 ka BP (*c*. AD 1200) (Figure 5). The period is also characterized by higher values of magnetic susceptibility (40–0 cm, Figure 2) which can be attributed to increasing occurrence of medium and coarse sand (Figure 4). The foraminiferal fauna is, to some extent, similar to the faunas prior to 3.2 ka BP, and may indicate the return to more favourable bottom-water conditions with an influx of saline (subsurface) WGC water of Atlantic (Irminger) origin to the fjord floor (M.-S. Seidenkrantz, S. Aagaard-Sørensen, H.S. Møller, A. Kuijpers, K.G. Jensen H. Kunzendorf, unpublished data 2006). The increase in sea-ice diatoms coincides with the occurrence of medium and coarse-grained sand, indicating a fall in surface-water temperatures and more extensive sea-ice formation. The scenario from 0.8 ka BP suggests pronounced water-mass stratification in the fjord, and may be attributed to changes in the oceanographic conditions in the WGC regime as well as decreased wind stress. Minimum values in Fe-intensity suggest that meltwater production reached a minimum during this period.

Palaeoclimatic implications

A schematic diagram of the inferred variances in the meltwater discharge based on suspended sediment input, the occurrence of sea ice and bottom water conditions (bwc) in Ameralik is shown in Figure 6a. The results are compared with Northern Hemisphere June insolation (W/m^2), reconstructed GRIP borehole temperatures (°C), August sea-surface temperature (SST) in the EGC on the East Greenland shelf and characteristic vegetation stages based on pollen analysis from Johs. Iversen Lake in the Godthaabsfjord interior (Fredskild, 1983; Berger and Loutre, 1991; Dahl-Jensen *et al*., 1998; Andersen

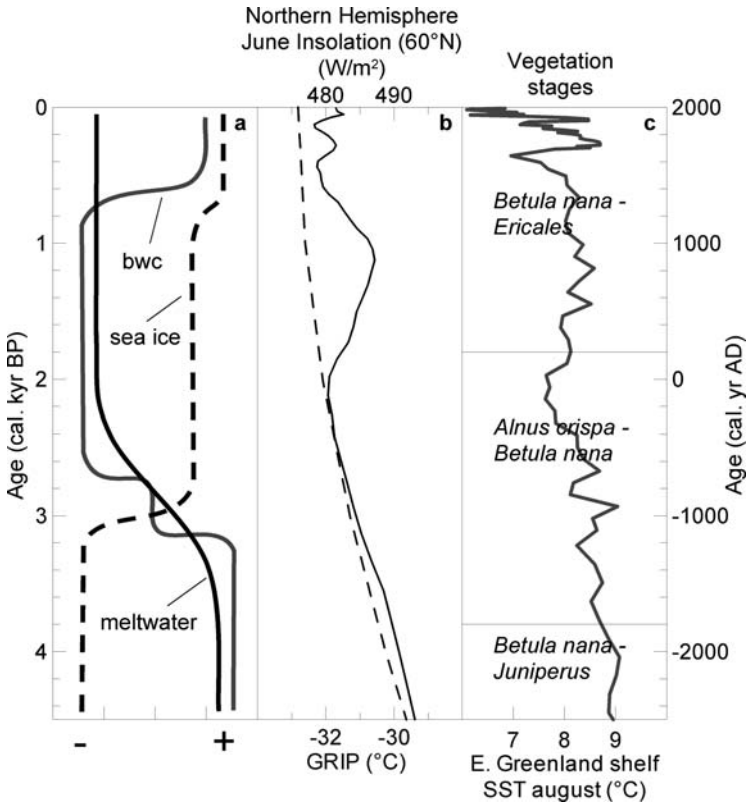

Figure 6 Schematic diagram of the influence from meltwater, the occurrence of sea ice and bottom water conditions (bwc) in Ameralik (a), with Northern Hemisphere June insolation (60°N) (Berger and Loutre, 1991) and reconstructed borehole temperatures from GRIP (°C) (full line) (Dahl-Jensen *et al.*, 1998) (b), August sea-surface temperature (SST) from the East Greenland Shelf (67°N) reconstructed from diatoms (Andersen *et al.*, 2004) and vegetation stages from lakes in the interior of Godthaabsfjord (Fredskild, 1983) (c)

et al., 2004). The decreasing meltwater supply and increasing occurrence of sea-ice-rafted material at 3.2 ka BP indicates millennial-scale atmospheric cooling in the area (Figure 6a). This overall cooling resulted in a shift in fjord type towards a more polar setting following the fjord type continuum suggested by Desloges *et al.* (2002).

The millennial-scale cooling trend corresponds to the long-term decrease in summer solar insolation at northern high latitudes (Berger and Loutre, 1991) and is reflected in the borehole palaeotemperature records from ice cores (Dahl-Jensen *et al.*, 1998). The shift in vegetation stages from *Betula nana – Juniperus*, which is considered to represent the warmest and driest period in this part of Greenland, to colder conditions during the *Betula nana – Ericales* stage also confirm a long-term change toward cooler conditions (Fredskild, 1983). The intermediate *Alnus crispa – Betula nana* stage is unique for the interior of the Godthaabsfjord region and the climate signal is unclear (Fredskild, 1985). The general agreement between the records illustrates how the interpreted changes in the fjord sedimentary environment follow both more regional terrestrial and large-scale marine palaeoclimatic records.

Atmospheric conditions in the region are closely related to the position of the low-pressure trough over Baffin Island, which has a major influence on the storm tracks and thereby the temperature and the distribution of precipitation (Williams and Bradley, 1985). An eastward displacement of the trough causes increased frequency in airflow from a northern direction, resulting in colder and generally drier summer conditions. A westward displacement leads to above-average summer temperatures and relatively mild winters because of more frequent 'warm' southerly winds (Williams and Bradley, 1985). The latter scenario may have prevailed in the HTM period prior to 3.2 ka BP.

Conclusions

The late-Holocene sedimentary record in the Ameralik Fjord is dominated by fine-grained sediment settling from a turbid surface plume with periodic admixtures of coarse-grained sea-ice-rafted and aeolian material. The period from the beginning of the record (at 4.4 ka BP) to 3.2 ka BP is characterized by high meltwater supply, originating from melting of the land-based glaciers caused by a relatively warm, and probably windy, climate and is concluded to mark the termination of the HTM (Figure 6).

From 3.2 ka BP to the present the sedimentation rate of fine-grained sediment is lower and there is a larger influence from sea-ice-rafted material indicating colder atmospheric conditions (Figure 6). This coincides with a poorer ventilation of bottom water masses in the fjord, which may be associated with increased stratification and sea-ice formation (Figure 6). The changes in the microfossil assemblages around 0.8 ka BP indicate increased influx of saline, subsurface WGC, while atmospheric conditions apparently remain cold. In addition, more extensive sea-ice formation after that time may further have been favoured by decreased wind activity.

The investigations demonstrate that sedimentary records from (west) Greenland fjords provide valuable palaeoclimatic information revealing links between local environmental conditions and large-scale North Atlantic ocean and atmospheric circulation patterns.

Acknowledgements

We thank Captain Gerhard Herzig and his crew on R/V *Alexander von Humboldt* for ship operations, chief scientist

Gerd Hoffmann-Wieck, GEOMAR, and shipboard technical and scientific staff for their engagement during the work at sea. John Boserup (GEUS) was an indispensable help during the cruise. For MSCL measurements we sincerely acknowledge the work by the late B. Schulz (IOW). Aad Vaars (Avaatech) as well as Rinike Gieles and Thomas Richter at the Royal Netherlands Institute for Sea Research assisted with XRF-scanning. Trine Dahl at University of Tromsø, Norway assisted with the X-radiographs. Holger Lindgren (GEUS) made the clay mineral analysis. The laboratory at Institute of Geography, University of Copenhagen helped with carbon and grain-size analyses. To all these people and institutions we offer our sincere thanks. We appreciate the review of an early version of the paper by R. Gilbert and two anonymous reviewers. The work was supported by University of Copenhagen, the EU PACLIVA project (No. EVK2-CT-2002-00143, GEUS) and the Danish Natural Science Council (No. 21-04-0336).

References

Andersen, C., Koc, N., Jennings, A.E. and **Andrews, J.T.** 2004: Nonuniform response of the major surface currents in the Nordic Seas to insolation forcing: implications for the Holocene climate variability. *Paleoceanography* 19, 1–16.

Andrews, J.T. and **Stravers, J.A.** 1993: Magnetic susceptibility of late Quaternary marine sediments, Frobisher Bay, N.W.T: an indicator of changes in provenance and processes. *Quaternary Science Reviews* 12, 157–67.

Andrews, J.T. and **Syvitski, J.P.M.** 1994: Sediment fluxes along high-latitude glaciated continental margins: northeast Canada and eastern Greenland. In Hay, W., editor, *Material fluxes on the surface of the earth*. National Academy Press, 99–115.

Andrews, J.T., Milliman, J.D., Jennings, A.E., Rynes, N. and **Dwyer, D.** 1994: Sediment thicknesses and Holocene glacial marine sedimentation rates in three east Greenland Fjords (ca. 68°N). *The Journal of Geology* 102, 669–83.

Ballantyne, C.K. 2002: Paraglacial geomorphology. *Quaternary Science Reviews* 21, 1935–2017.

Bennike, O. 2004: Holocene sea-ice variations in Greenland: onshore evidence. *The Holocene* 14, 607–13.

Berger, A. and **Loutre, M.F.** 1991: Insolation values for the climate of the last 10 million years. *Quaternary Science Reviews* 10, 297–317.

Bronk Ramsey, C. 2001: Development of the radiocarbon calibration program. *Radiocarbon* 43, 355–63.

Buch, E., 2000: *A monograph on the physical oceanography of Greenland waters.* Report no. 00-12. Danish Meteorological Institute.

Cappelen, J., Jørgensen, B.V., Laursen, E.V., Stannius, L.S. and **Thomsen, R.S.** 2001: *The observed climate of Greenland, 1958–99 – with climatological standard normals, 1961–90.* Report no. 00-18. DMI, Danish Meteorological Institute.

Cuffey, K.M. and **Clow, G.D.** 1997: Temperature, accumulation, and ice sheet elevation in central Greenland through the last deglacial transition. *Journal of Geophysical Research – Oceans* 102, 26 383–96.

Cuny, J., Rhines, P.B., Niiler, P.P. and **Bacon, S.** 2002: Labrador Sea boundary currents and the fate of Irminger Sea Water. *Journal of Physical Oceanography* 32, 627–47.

Dahl-Jensen, D., Mosegaard, K., Gundestrup, N., Clow, G.D., Johnsen, S.J., Hansen, A.W. and **Balling, N.** 1998: Past temperatures directly from the Greenland Ice Sheet. *Science* 282, 268–71.

Desloges, J.R., Gilbert, R., Nielsen, N., Christiansen, C., Rasch, M. and **Øhlenschlæger, R.** 2002: Holocene glacimarine sedimentary environments in fiords of Disko Bugt, West Greenland. *Quaternary Science Reviews* 21, 947–63.

Domack, E., Leventer, A., Root, S., Ring, J., Williams, E., Carlson, D., Hirshorn, E., Wright, W., Gilbert, R. and **Burr, G.** 2003: Marine sedimentary record of natural environmental variability and recent warming in the Antarctic Peninsula. *Antarctic Research Series* 79, 205–24.

Evans, J., Dowdeswell, J.A., Grobe, H., Niessen, F., Stein, R., Hubberten, H.-W. and **Whittington, R.J.** 2002: Late Quaternary sedimentation in Kejser Franz Joseph Fjord and the continental margin of East Greenland. In Dowdeswell, J.A. and Ó'Cofaigh, C., editors, *Glacier-influenced sedimentation on high-latitude continental margins.* The Geological Society of London, 149–79.

Forbes, D.L. and **Syvitski, J.P.M.** 1994: Paraglacial coasts. In Carter, R.W.G. and Woodroffe, C.D., editors, *Coastal evolution: late quaternary shoreline morphodynamics.* Cambridge University Press, 373–424.

Fredskild, B. 1983: *The Holocene vegetational development of the Godthåbsfjord area, West Greenland.* Meddelelser om Grønland, Geoscience, 10, 1–28.

—— 1985: Holocene pollen records from west Greenland. In Andrews, J.T., editor, *Quaternary environments, eastern Canadian Arctic, Baffin Bay and Western Greenland.* Allen & Unwin, 643–81.

Funder, S. 1989: Quaternary geology of the ice-free areas and adjacent shelves of Greenland. In Fulton, R.J., editor, *Quaternary geology of Canada and Greenland.* Geological Survey of Canada, 743–92.

Funder, S. and **Fredskild, B.** 1989: Paleofaunas and floras (Greenland). In Fulton, R.J., editor, *Quaternary geology of Canada and Greenland.* Geological Survey of Canada, Geology of Canada, 775–83.

Gilbert, R. 1983: Sedimentary processes of Canadian arctic fjords. *Sedimentary Geology* 36, 147–75.

—— 1990: Rafting in glacimarine environments. In Dowdeswell, J.A. and Scourse, J.D., editors, *Glacimarine environments: processes and sediment.* The Geological Society, 105–20.

—— 2000: Environmental assessment from the sedimentary record of high-latitude fiords. *Geomorphology* 32, 295–314.

Gilbert, R., Nielsen, N., Desloges, J.R. and **Rasch, M.** 1998: Contrasting glacimarine sedimentary environments of two arctic fiords on Disko, West Greenland. *Marine Geology* 147, 63–83.

Gilbert, R., Nielsen, N., Moller, H., Desloges, J.R. and **Rasch, M.** 2002: Glacimarine sedimentation in Kangerdluk (Disko Fjord), West Greenland, in response to a surging glacier. *Marine Geology* 191, 1–18.

Hald, M. and **Korsun, S.** 1997: Distribution of modern benthic foraminifera from fjords of Svalbard, European Arctic. *Journal of Foraminiferal Research* 27, 101–22.

Hald, M., Husum, K., Vorren, T.O., Grosfjeld, K., Jensen, H.B. and **Sharapova A.** 2003: Holocene climate in the subarctic fjord Malangen, northern Norway: a multi-proxy study. *Boreas* 32, 543–59.

Jansen, J.H.F., Van der Gaast, S.J., Koster, B. and **Vaars, A.J.** 1998: CORTEX, a shipboard XRF-scanner for element analyses in split sediment cores. *Marine Geology* 151, 143–53.

Jennings, A.E. and **Helgadottir, G.** 1994: Foraminiferal assemblages from the fjords and shelf of eastern Greenland. *Journal of Foraminiferal Research* 24, 123–44.

Jennings, A.E. and **Weiner, N.J.** 1996: Environmental change in eastern Greenland during the last 1300 years: evidence from foraminifera and lithofacies in Nansen Fjord, 68 degrees N. *The Holocene* 6, 179–91.

Jennings, A.E., Knudsen, K.L., Hald, M., Hansen, C.V. and **Andrews, J.T.** 2002: A mid-Holocene shift in Arctic sea-ice variability on the East Greenland Shelf. *The Holocene* 12, 49–58.

Jensen, K.G., Kuijpers, A., Koc, N. and **Heinemeier, J.** 2004: Diatom evidence of hydrographic changes and ice conditions in Igaliku Fjord, South Greenland, during the past 1500 years. *The Holocene* 14, 152–65.

Kaplan, M.R., Wolfe, A.P. and **Miller, G.H.** 2002: Holocene environmental variability in southern Greenland inferred from lake sediments. *Quaternary Research* 58, 149–59.

Kaufman, D.S., Ager, T.A., Anderson, N.J., Anderson, P.M., Andrews, J.T., Bartlein, P.J., Brubaker, L.B., Coats, L.L., Cwynar, L.C. and **Duvall, M.L.** 2004: Holocene thermal maximum in the western Arctic (0–180°W). *Quaternary Science Reviews* 23, 529–60.

Kelly, M. 1980: The status of the Neoglacial in western Greenland. *The Geological Survey of Greenland Report* 96, 1–26.
Kerwin, M.W., Overpeck, J.T., Webb, R.S. and **Anderson, K.H.** 2004: Pollen-based summer temperature reconstructions for the eastern Canadian boreal forest, subarctic, and Arctic. *Quaternary Science Reviews* 23, 1901–24.
Lassen, S.J., Kuijpers, A., Kunzendorf, H., Hoffmann-Wieck, G., Mikkelsen, N. and **Konradi, P.** 2004: Late-Holocene Atlantic bottom-water variability in Igaliku Fjord, South Greenland, reconstructed from foraminifera faunas. *The Holocene* 14, 165–71.
Lloyd, J.M., Park, L.A., Kuijpers, B. and **Moros, M.** 2005: Early holocene palaeoceanography and deglacial chronology of Disko Bugt, West Greenland. *Quaternary Science Reviews* 24, 1741–55.
Long, A.J., Roberts, D.H. and **Rasch, M.** 2003: New observations on the relative sea level and deglacial history of Greenland from Innaarsuit, Disko Bugt. *Quaternary Research* 60, 162–71.
Lyså, A., Sejrup, H.P. and **Aarseth, I.** 2004: The late glacial–Holocene seismic stratigraphy and sedimentary environment in Ranafjorden, northern Norway. *Marine Geology* 211, 45–78.
Marienfeld, P. 1992: Recent sedimentary processes in Scoresby Sund, East Greenland. *Boreas* 21, 105–92.
McGregor, V.R. 1993: *Descriptive text to 1:100 000 map, sheet Qôrqut 64 V.1 Syd*. Grønlands Geologiske Undersøgelse.
Morehead, M.D., Syvitski, J.P. and **Hutton, E.W.H.** 2001: The link between abrupt climate change and basin stratigraphy: a numerical approach. *Global and Planetary Change* 28, 107–27.
Neuman, C.M. 1993: A review of aeolian transport processes in cold environments. *Progress in Physical Geography* 17, 137–55.
O'Cofaigh, C. and **Dowdeswell, J.A.** 2001: Laminated sediments in glacimarine environments: diagnostic criteria for their interpretation. *Quaternary Science Reviews* 20, 1411–36.
O'Cofaigh, C., Dowdeswell, J.A. and **Grobe, H.** 2001: Holocene glacimarine sedimentation, inner Scoresby Sund, East Greenland: the influence of fast-flowing ice-sheet outlet glaciers. *Marine Geology* 175, 103–29.
Øhlenschlæger R. 2000: Recente foraminiferers fordeling og Sen-Holocæne klimavariationer fra fjordsystemer i det centrale Vestgrønland. Unpublished Ms. Thesis. Maringeologisk Afdeling, Geologisk Institut, Aarhus Universitet.
Polyak, L., Korsun, S., Febo, L.A., Stanovoy, V., Khusid, T., Hald, M., Paulsen, B.E. and **Lubinski, D.J.** 2002: Benthic foraminiferal assemblages from the southern Kara Sea, a river-influenced Arctic marine environment. *Journal of Foraminiferal Research* 32, 252–73.
Prins, M.A., Troelstra, S.R., Kruk, R.W., van der Borg, K., de Jong, A.F.M. and **Weltje, G.J.** 2001: The late Quaternary sedimentary record of Reykjanes Ridge, North Atlantic. *Radiocarbon* 43, 939–47.
Rasch, M. 2000: Holocene relative sea level changes in Disko Bugt, West Greenland. *Journal of Coastal Research* 16, 306–15.
Roussell, A. 1936: Sandnes and the neighbouring farms. *Meddelelser om Grønland* 88, 1–222.
Sejrup, H.P., Haflidason, H., Flatebo, T., Kristensen, D.K., Grosfjeld, K. and **Larsen, E.** 2001: Late-glacial to Holocene environmental changes and climate variability: evidence from Voldafjorden, western Norway. *Journal of Quaternary Science* 16, 181–98.
Steenfelt, A. 1990: *Regional compilations of geoscience data from the Nuuk-Manitsoq area, Southern West Greenland*. GGU. Thematic Map Series.
Steinsund, P.I. 1994: Distribution of calcareous benthic foraminifera in recent sediments of the Barents and Kara Sea. Ph.D. Thesis. Department of Geology, Institute of Biology and Geology, University of Tromsø.
Stoner, J.S. and **Andrews, J.T.** 1999: The North Atlantic as a Quaternary magnetic archive. In Maher, B.A. and Thompson, R., editors, *Quaternary climates, environments and magnetism*. Cambridge University Press, 49–80.
Stravers, J.A., Syvitski, J.P.M. and **Praeg, D.B.** 1991: Application of size sequence data to glacial-paraglacial sediment transport and sediment partitioning. In Syvitski, J.P.M., editor, *Principles, methods, and application of particle size analysis*. Cambridge University Press, 293–310.
Stuiver, M., Reimer, P.J. and **Braziunas, T.F.** 1998: High-precision radiocarbon age calibration for terrestrial and marine samples. *Radiocarbon* 40, 1127–51.
Syvitski, J.P.M. 2002: Sediment discharge variability in Arctic rivers: implications for a warmer future. *Polar Research* 21, 323–30.
Syvitski, J.P.M., Burrel, D.C. and **Skei, J.M.** 1987: *Fjords processes and products*. Springer-Verlag.
Syvitski, J.P., LeBlanc, K.W.G. and **Cranston, R.E.** 1990: The flux and preservation of organic carbon in Baffin Islands fjords. In Dowdeswell, J.A. and Scourse, J.D., editors, *Glacimarine environments: processes and sediments*. The Geological Society, 177–200.
Syvitski, J.P.M., Andrews, J.T. and **Dowdeswell, J.A.** 1996: Sediment deposition in an iceberg-dominated glacimarine environment, East Greenland: basin fill implications. *Global and Planetary Change* 12, 251–70.
Taurisano, A., Bøggild, C.E. and **Karlsen, H.** 2004: A century of climate variability and climate gradients from coast to ice sheet in West Greenland. *Geografiska Annaler – Series A – Physical Geography* 86, 217–25.
Telford, R.J., Heegaard, E. and **Birks, H.J.B.** 2004: The intercept is a poor estimate of a calibrated radiocarbon age. *The Holocene* 14, 296–98.
van de Flierdt, T., Hemming, S.R. and **Goldstein, S.L.** 2005: Effects of continental weathering and sedimentary sorting on the Hf, Nd, and Pb isotopic composition of sediments and implications for dissolved input to the ocean. *Eos Transactions of the American Geophysical Union* 86, Joint Assembly Supplement, Abstract PP23A-05.
Vinther, B.M., Johnsen, S. and **Clausen, H.B.** 2005: *Central Greenland late Holocene temperatures*. EGU General Assembly, Vienna, Geophysical Research Abstracts 7.
Weber, M.E., Niessen, F., Kuhn, G. and **Wiedicke, M.** 1997: Calibration and application of marine sedimentary physical properties using a multi-sensor core logger. *Marine Geology* 136, 151–72.
Weidick, A. 1978: *Quaternary map of Greenland, Frederikshåb Isblink – Søndre Strømfjord*. Geodetic Institute.
—— 1993: Neoglacial change of ice cover and the related response of the Earth's crust in West Greenland. *Grønlands Geologiske Undersøgelser Rapport* 159, 121–26.
Weidick, A. and **Olesen, O.B.** 1980: Hydrological basins in West Greenland. *Grønlands Geologiske Undersøgelser* Report 94.
Weltje, G.J. 1997: End-member modelling of compositional data: numerical-statistical algorithms for solving the explicit mixing problem. *Mathematical Geology* 29, 503–49.
Weltje, G.J. and **Prins, M.A.** 2003: Muddled or mixed? Inferring palaeoclimate from size distributions of deep-sea clastics. *Sedimentary Geology* 162, 39–62.
Willemse, N.W., Koster, E.A., Hoogakker, B. and **van Tatenhove, F.G.M.** 2003: A continuous record of Holocene eolian activity in West Greenland. *Quaternary Research* 59, 322–34.
Williams, L.D. and **Bradley, R.S.** 1985: Paleoclimatology of the Baffin Bay region. In Andrews, J.T., editor, *Quaternary environments of eastern Canadian Arctic, Baffin Bay and Western Greenland*. Allen and Unwin, 741–72.
Winters, G.V. and **Syvitski, J.P.M.** 1992: Suspended sediment character and distribution in McBeth Fjord, Baffin Island. *Arctic* 45, 25–35.